A&A 543, A86 (2012)
DOI: 10.1051/0004-6361/201118315

Astronomy & Astrophysics

Five-year optical and near-infrared observations of the extremely slow nova V1280 Scorpii⋆,⋆⋆

H. Naito[1], S. Mizoguchi[2], A. Arai[3], A. Tajitsu[4], S. Narusawa[5], M. Yamanaka[6], M. Fujii[7], T. Iijima[8], K. Kinugasa[9], M. Kurita[1], T. Nagayama[1], H. Yamaoka[10], and K. Sadakane[11]

[1] Graduate School of Science, Nagoya University, Furo-cho, Chikusa-ku, 464-8602 Nagoya, Japan
e-mail: naito@stelab.nagoya-u.ac.jp
[2] Sendai Astronomical Observatory, Nishikigaoka, Aoba-ku, 989-3123 Sendai, Japan
[3] Koyama Astronomical Observatory, Kyoto Sangyo University, Motoyama, Kamigamo, Kita-ku, 603-8555 Kyoto, Japan
[4] Subaru Telescope, National Astronomical Observatory of Japan, 650 North A'ohoku Place, Hilo, HI 96720, USA
[5] Nishi-Harima Astronomical Observatory, Sayo-cho, 679-5313 Hyogo, Japan
[6] Hiroshima Astrophysical Science Center, Hiroshima University, Kagamiyama, Higashi-Hiroshima, 739-8526 Hiroshima, Japan
[7] Fujii Bisei Obsevatory, Kurosaki, Tamashima, Kurashiki, 713-8126 Okayama, Japan
[8] Astronomical Observatory of Padova, Asiago Section, Osservatorio Astrofisico, 36012 Asiago (Vi), Italy
[9] Gunma Astronomical Observatory, Agatsuma-gun, 377-0702 Gunma, Japan
[10] Graduate School of Sciences, Kyushu University, Hakozaki, Higashi-ku, 812-8581 Fukuoka, Japan
[11] Astronomical Institute, Osaka Kyoiku University, Asahigaoka, Kashiwara, 582-8582 Osaka, Japan

Received 21 October 2011 / Accepted 30 March 2012

ABSTRACT

We present optical (B, V, R_c, I_c and y) and near-infrared (J, H, and K_s) photometric and spectroscopic observations of a classical nova V1280 Scorpii for five years from 2007 to 2011. Our photometric observations show a declining event in optical bands shortly after the maximum light, which took about 250 days to recover. This event was most probably caused by dust formation. The event was accompanied by a short (~30 days) re-brightening episode (~2.5 mag in V), which suggests that there had been some re-ignition of the surface nuclear burning. After 2008, the y band observations show a very long plateau at around $y = 10.5$ for more than 1000 days until April 2011 (~1500 days after the maximum light). The nova had taken a very long time (~50 months) to enter the nebular phase, according to a clear detection of both [O III] 4959 and 5007 and is still continuing to generate the wind caused by H-burning. This finding suggests that historically V1280 Sco is evolving at its slowest ever measured rate. The interval from the maximum light (2007 February 16) to the beginning of the nebular phase is longer than any previously known slow novae: V723 Cas (18 months), RR Pic (10 months), or HR Del (8 months). It suggests that the mass of a white dwarf in the V1280 Sco system might be 0.6 $M_\odot$ or lower. The distance, based on our measurements of the expansion velocity combined with the directly measured size of the dust shell, is estimated to be 1.1 ± 0.5 kpc.

Key words. stars: individual: V1280 Sco – novae, cataclysmic variables – stars: abundances – stars: distances

1. Introduction

It has been widely accepted that a classical nova occurs as a result of thermonuclear runaway in a close binary system consisting of a white dwarf (WD) and a normal star, when material accreted onto the WD bursts as it reaches the critical mass limit (e.g. Warner 1995; Bode & Evans 2008). Novae are classified according to the decline rate and their spectroscopic features. In the General Catalogue of Variable Stars (Samus et al. 2004), the parameter t_3 (number of days for a nova to decline three magnitudes from the maximum brightness) is used to classify the speed class based on the decline rate. When a nova is observed to have $t_3 < \sim 100$ days, it is classified as a fast nova, while when a nova has $t_3 \geq 150$ days, it is classified as a slow nova. Williams (1992) introduced two spectral classes, Fe II type and He/N type, using early post-outburst spectra. Fe II type novae are characterized by prominent Fe II and other lower ionization lines with P Cygni absorption components and display a slow spectral evolution. On the other hand, He/N type novae have strong He, N, and other high ionization lines, high expansion velocities, and a very rapid spectral evolution. Slow novae tend to be Fe II type novae, whereas He/N novae are found only among the fast class.

For a long time, there had been a problem in establishing which parameters (the WD mass, the WD magnetic field strength, the composition of the WD envelope, and the accretion rate) can be used to determine the nova type. This was partly solved by the discovery of a universal decline law of classical novae by Hachisu & Kato (2006). They found that the speed class is mainly determined by the mass of a WD, when the optically thick wind is taken into account (Friedjung 1966; Kato & Hachisu 1994). However, it is still difficult for any of their models to predict observed photometric behaviors near the optical peak and to describe any type of complex spectral evolution, because the model is only effective during the late (quietly) declining phase, when the flux originates mainly from the extended region emitting the free-free radiation. To understand all of the physical processes involved in a nova explosion, it is important

⋆ Tables 2, 3, and 5 and Figs. 7, 8, 10, and 12 are available in electronic form at http://www.aanda.org

⋆⋆ Reduced data is only available at the CDS via anonymous ftp to cdsarc.u-strasbg.fr (130.79.128.5) or via http://cdsarc.u-strasbg.fr/viz-bin/qcat?J/A+A/543/A86

Table 1. List of observatories.

Photometry Observatory	Telescope	Band	Instrument	Observation period	Nights
OKU	0.51-m reflector	y, B, V, R_c, I_c		February 2007–April 2011	133
SAAO	1.4-m IRSF telescope	J, H, Ks	SIRPOL (1)	July 2009–August 2010	2
Spectroscopy Observatory	**Telescope**	**Resolution**	**Instrument**	**Observation period**	**Nights**
NHAO	2.0-m NAYUTA telescope	Medium	MALLS (2)	February 2007–September 2008	23
FBO	0.28-m reflector	Low		February 2007–February 2008	13
BAO	1.01-m telescope	Medium		April 2009	1
Subaru	8.2-m Subaru telescope	High	HDS (3)	May 2009–July 2011	9
GAO	1.5-m telescope	Low	GLOWS	June 2009–June 2010	5
HHAO	1.5-m KANATA telescope	Low	HOWPol (4)	March 2010–August 2010	3
KAO	1.3-m ARAKI telescope	Low	LOSA/F2	July 2010	1
Asiago	1.22-m telescope	Medium	Boller & Chivens	April 2011	1

Notes. OKU: Osaka Kyoiku University, SAAO: South African Astronomical Observatory, NHAO: Nishi-Harima Astronomical Observatory, FBO: Fujii Bisei Observatory, BAO: Bisei Astronomical Observatory, Subaru: Subaru Telescope, GAO: Gunma Astronomical Observatory, HHAO: Higashi-Hiroshima Astronomical Observatory, KAO: Koyama Astronomical Observatory, Asiago: Asiago Astrophysical Observatory.

References. (1) SIRPOL: Kandori et al. (2006), (2) MALLS: Ozaki & Tokimasa (2005), (3) HDS: Noguchi et al. (2002), (4) HOWPol: Kawabata et al. (2008).

to observe from the very early phase including the pre-maximum to the late declining phase over a long period of time. In this respect, a very slow nova provides us with a rare opportunity to follow its evolution closely.

V1280 Sco (Nova Scorpii 2007 No. 1) is a classical nova that was discovered independently by Nakamura and Sakurai on the same night (2007 February 4) at ninth visual magnitude (Yamaoka et al. 2007a). Its early spectra were taken by some observers (e.g. Naito & Narusawa 2007; Kuncarayakti et al. 2008) and it was classified as an Fe II type nova (Munari et al. 2007). Yamaoka et al. (2007c) reported that its spectrum at the pre-maximum stage resembled that of an F-type supergiant dominated by absorption lines of hydrogen, Fe II, and other metals. It followed a somewhat slow rise to its maximum brightness of $V = 3.78$ mag on February 16, which was 11.3 days after its discovery (Munari et al. 2007), and since the discovery of both V382 Vul and V1494 Aql in 1999, it has become a naked eye nova. Hounsell et al. (2010) published the data set of V1280 Sco observed by the Solar Mass Ejection Imager (SMEI) on board the *Coriolis* satellite. Thanks to the high time resolution, they revealed that there had been three major but short episodes of brightening before February 20, which had not been detected by ground-based observers. More notably, this nova showed a remarkable formation of dust in its very early phase (Das et al. 2007). After maximum light, it faded steadily for about 12 days, before undergoing a precipitous decline in visual magnitude caused by dust formation, that was directly detected by Chesneau et al. (2008) via the Very Large Telescope Interferometer near-infrared (NIR) and mid-infrared observations. Das et al. (2008) suggested that the dust was in clumps from NIR studies of V1280 Sco. Owing to dust formation, the parameter t_3 is not applicable as an indicator of the speed class in the case of V1280 Sco.

Hounsell et al. (2010) estimated the distance of V1280 to be 630 ± 100 pc by measuring the condensation time of dust grains from SMEI results, assuming that the condensation temperature of the dust was 1200 K and the ejection velocity about 600 km s^{-1}. On the other hand, Chesneau et al. (2008) derived the distance of 1.6 ± 0.4 kpc from direct observations of the size of the expanding shell. The discrepancy between these two estimations of distance is over a factor of two, which could result from the complexity in the physical conditions (temperature and velocity) of the dust shell.

In this paper, we present the results of our long-term multi-band photometry and low, medium, and high dispersion spectroscopy spanning over five years from 2007 to 2011. Our observations are summarized in Sect. 2. Light curves and spectral evolutions are described in Sects. 3 and 4, respectively. We discuss the distance, the WD mass, and the ejected mass of V1280 Sco in Sect. 5 and a summary is given in Sect. 6.

2. Observations

The list of observatories used to acquire data analyzed in this study is tabulated in Table 1.

2.1. Photometry

We conducted B, V, R_c, I_c, and y band photometric observations using a CCD camera mounted on the 0.51-m reflector at Osaka Kyoiku University (OKU) from February 2007 to April 2011. The field of view of the camera was 10′ × 16′. We obtained differential magnitudes of the object relative to a comparison star using aperture photometry derived with the APPHOT package in IRAF[1]. We selected a nearby star, HD 152819 (B4 IV), as a comparison star. Its magnitudes of $B = 9.951 \pm 0.049$, $V = 9.935 \pm 0.069$, $R_c = 9.878 \pm 0.058$, and $I_c = 9.847 \pm 0.039$ were quoted from Henden & Munari (2007). The log of the optical photometric observations and the derived B, V, R_c, I_c, and y magnitudes with errors are given in Table 2.

Our optical photometric monitoring is characterized by using an intermediate-band y filter, whose wavelength coverage (530–560 nm; produced by Custom Scientific, Inc.[2]) is almost free from contamination by the emission lines of novae related mainly to Fe II during the early stage of evolution of the nova and [N II] 5755 and [O III] 4959 and 5007 in its late stage (nebular phase). The y-band observations have been promoted by Kato and Hachisu to obtain y light curves representing the continuum

[1] IRAF is distributed by NOAO for Research in Astronomy, Inc., under cooperative agreement with the National Science Foundation.

[2] See http://www.customscientific.com

fluxes of novae for which their modeled light curves can be fitted to determine the WD mass (e.g. Hachisu et al. 2006; Hachisu & Kato 2007; Hachisu et al. 2008). The y magnitudes were measured by comparing with the V magnitude of the comparison star ($V = y = 9.935 \pm 0.069$) following Crawford (1987). The difference between the y and V magnitudes reflects a contamination by emission lines of the continuum observed through the wide-passband of V.

Our J, H, and K_s band photometric observations were performed with the SIRPOL (SIRius POLarimeter) mounted on the 1.4-m IRSF telescope at the South African Astronomical Observatory (SAAO) in 2009 and 2010. The field of view of the SIRPOL camera was $7\farcm7 \times 7\farcm7$. We obtained NIR magnitudes by comparing to those of 2MASS catalog stars in the same frame field-of-view using the APPHOT package in IRAF; 2MASS 16 573 775-3 221 553 ($J = 8.291 \pm 0.027$, $H = 7.683 \pm 0.071$ and $K = 7.481 \pm 0.018$), 2MASS 16 573 563-3 219 050 ($J = 9.062 \pm 0.026$, $H = 8.192 \pm 0.053$ and $K = 7.832 \pm 0.029$), 2MASS 16 574 251-3 218 242 ($J = 8.885 \pm 0.020$, $H = 8.056 \pm 0.061$ and $K = 7.744 \pm 0.031$) and 2MASS 16 575 182-3 222 448 ($J = 7.772 \pm 0.021$, $H = 6.870 \pm 0.042$ and $K = 6.547 \pm 0.029$) were used (Cutri et al. 2003).

2.2. Spectroscopy

Low-dispersion spectroscopic observations from 2007 to 2008 were carried out using a spectrograph mounted on the 0.28-m telescope at Fujii Bisei Observatory (FBO). The spectral resolution was $R = \lambda/\Delta\lambda \cong 600$ at Hα. Low-dispersion spectroscopic observations from 2009 to 2010 were carried out using different combinations of 1-m class telescopes and spectrographs, namely the GLOWS (Gunma LOW resolution Spectrograph and imager) mounted on the 1.5-m telescope at Gunma Astronomical Observatory (GAO), the HOWPol (Hiroshima One-shot Wide-field Polarimeter) mounted on the 1.5-m KANATA telescope at Higashi-Hiroshima Astronomical Observatory (HHAO) of Hiroshima University, and the LOSA/F2 mounted on the 1.3-m ARAKI telescope at Koyama Astronomical Observatory (KAO) of Kyoto Sangyo University. The spectral resolutions at Hα for GLOWS, HOWPol, and LOSA/F2 were $R \cong 500$, 400, and 600, respectively.

Medium-dispersion spectroscopic observations were carried out using three instruments, the MALLS (Medium And Low dispersion Long slit Spectrograph) mounted on the 2.0-m NAYUTA telescope at Nishi-Harima Astronomical Observatory (NHAO) from 2007 to 2008, a spectrograph mounted on the 1.01-m telescope at Bisei Astronomical Observatory (BAO) in 2009, and the Boller & Chivens grating spectrograph mounted on the 1.22-m telescope at Asiago Astrophysical Observatory in 2011. The spectral resolutions at Hα were $R \cong 1200$ for these three instruments.

High-dispersion spectroscopic observations were carried out using the HDS (High Dispersion Spectrograph) mounted on the 8.2-m Subaru telescope from 2009 to 2011. The technical details of the HDS were described in Noguchi et al. (2002). The observational mode was the same as that used in Sadakane et al. (2010), which provided the resolving power at Hα of $R \cong 60\,000$ and covered the wavelength region from 4130 Å to 6860 Å.

A journal of spectroscopic observations of V1280 Sco is given in Table 3. Spectral data, except for those obtained at FBO and BAO, were reduced in a standard manner with the NOAO IRAF package. Spectrophotometric calibrations were performed using the spectra of standard stars: HR 1544, HR 3454, HR 4468, HR 4963, HR 5501, HR 6354, HR 7950, HR 7596, HR 8634, HR 9087, and HD 117 880 observed on the same nights. To carry out the final flux calibration on each night, we used the linearly interpolated y-band magnitude evaluated for two consecutive data points obtained before and after the date of each spectroscopic observation. This is because our raw spectroscopic data were affected by the large uncertainties in the absolute fluxes of both the target and standard stars due to the slit loss caused by a telescope guiding error and varying weather and seeing conditions during spectroscopic observations. We used the translation function between the absolute flux and the y magnitude given in Gray (1998). Errors in the flux were reduced to ∼10% by using this method. We used the value of $E(B-V) = 0.4$ to correct for the interstellar extinction, which was obtained by dividing $A_v = 1.2$ (from Das et al. 2008) by the assumed total-to-selective extinction ratio $R_v = 3.1$.

3. Light curves

The light curves and color indices for data acquired at optical wavelengths and NIR light curves are shown in Fig. 1. For convenience, we superimpose these data on the NIR light curves in the early phase published by Das et al. (2008). We set $t = 0$ d on 2007 February 16 (=JD 2 454 147.69), where t is the time in days from the maximum brightness (Munari et al. 2007). Photometric errors in magnitudes are typically smaller than 0.07 mag.

Figure 2 shows the V-band light curve during the initial phase (from $t = -13$ d to 37 d). We plot OKU V-band data together with the SMEI data (Hounsell et al. 2010), supplemented by several points quoted from IAU Circulars (Yamaoka et al. 2007a,b). The OKU V-band data show good agreement with the SMEI data expect for $t > 20$ d ($V > 10$), when the SMEI observations become uncertain because of SMEI's low sensitivity. As noted in Sect. 1, there are three short episodes (<1 d) of brightening with amplitudes of ∼1 mag near the peak. In this paper, we refer to them as "peak fluctuations".

After its discovery on 2007 February 4 ($t = -11.3$ d), the nova gradually increased its brightness to $V = 6.3$ within one week (the initial rising phase), then remained at its pre-maximum halt stage brightness for about two days. Thereafter, it reached its maximum brightness at $V_{max} = 3.78$ on 2007 February 16 ($t = 0$ d), and underwent the peak fluctuations described above. About two weeks after the maximum, the nova entered a rapid declining phase in V-band until late May 2007.

It is interesting to find that the nova remained nearly at the same brightness in K-band ($K \sim 4$) during the rapid decline (Fig. 3), and at the same time showed sudden increases in color indices $\Delta(V-R) \sim 1.0$ and $\Delta(V-I) \sim 1.5$ as shown in Fig. 1. From these results, we conclude that the rapid fading spanning from early March to May 2007 had been triggered by the dust formation in the ejecta reported by Chesneau et al. (2008) and Das et al. (2008). However, in view of the relatively small changes in the observed color indices such as $V - I$ compared to the sharp decline in the optical band ($\Delta V \sim 10$ within 80 days), we suspect that the observed decline cannot be accounted for by the dust obscuration alone. The decline might have been partly caused by the shrinking of the photosphere. The clumpy nature of the dust shells as suggested by Das et al. (2008) might be an important factor in accounting for the relatively small changes in the color indices.

In late May 2007 ($t \sim 100$ d), the first remarkable re-brightening in V-band occurred. During the rising phase, the object showed simultaneous brightenings in the J, H, and K bands (Das et al. 2008). During the second re-brightening phase from

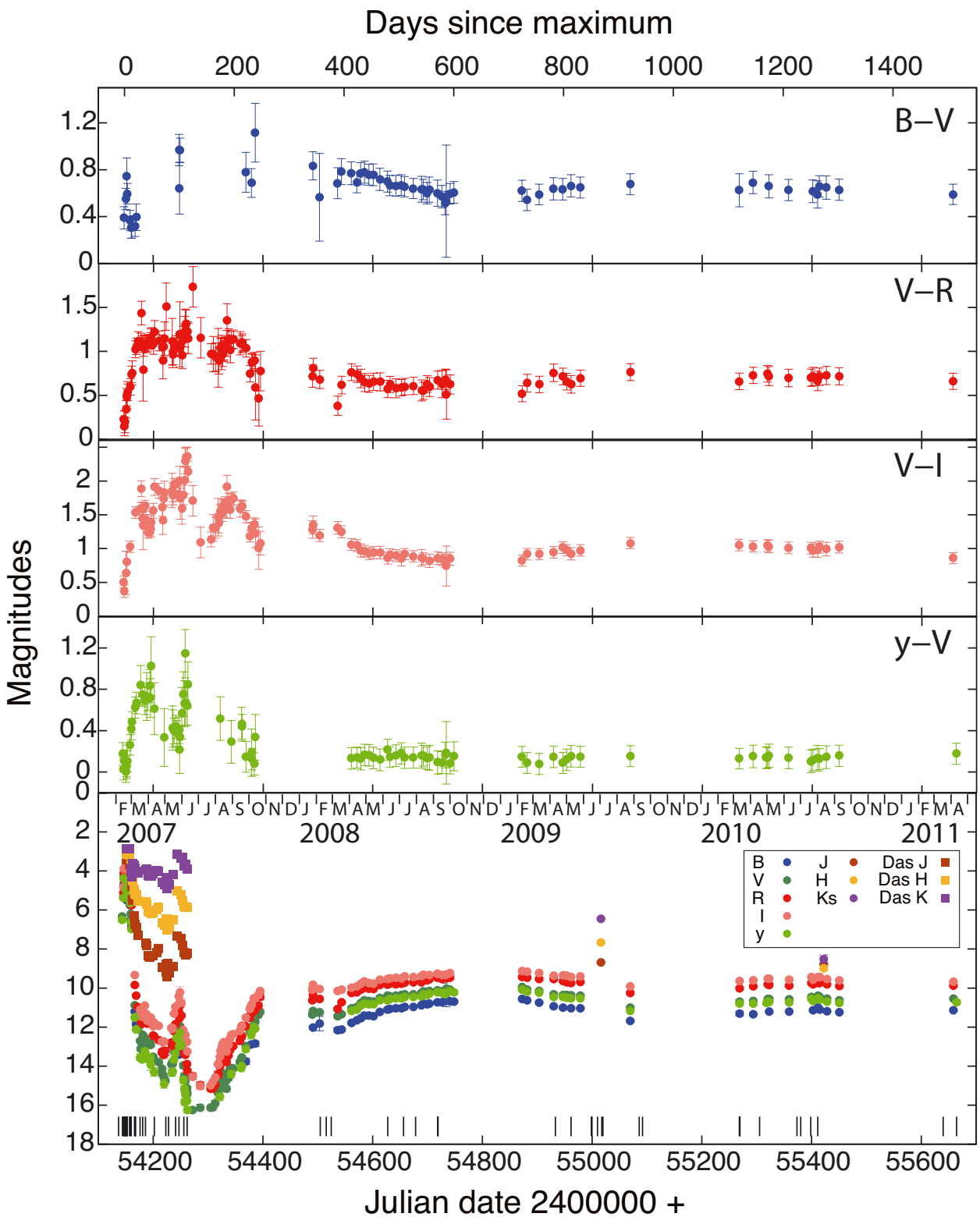

Fig. 1. Light curves in optical B, V, R_c, I_c, and y and NIR J, H, and K_s bands and color indices spanning five years. Dates of the spectroscopic observations are indicated by vertical lines.

August 2007 to October 2007, V1280 Sco was too faint to be observed through the B and y filters at OKU for about two months (from t = 140 d to 200 d). This implies that the V-band flux during this period came mainly from emission lines. The observation in the y band had recovered by around t = 200 d, and the index $y - V$ decreased from ~0.5 to ~0.2 within 50 days. This means that the continuum radiation had returned to its dust-free flux level in October 2007. At the same time, the color index $V-I$ increased from 1.1 to 1.7 (from t = 140 d to 200 d) and then decreased to 1.1 at t = 250 d. Analogous behaviors have been observed in many dust-forming novae (e.g. V475 Sct, Chochol et al. 2005), which have been interpreted as the result of the dust

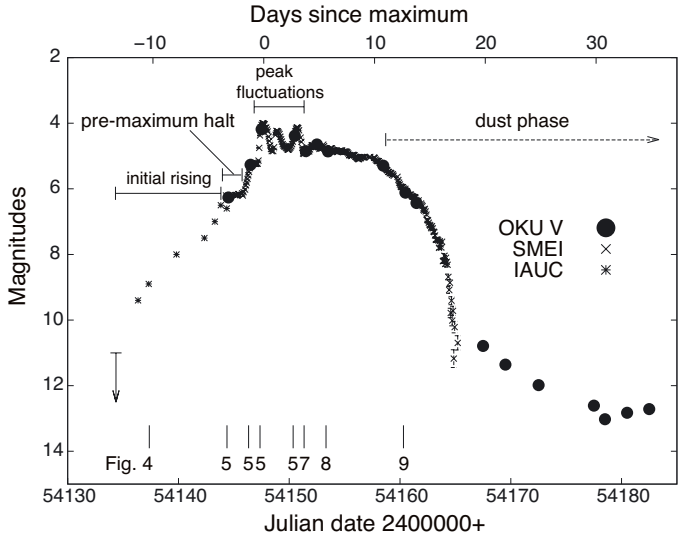

Fig. 2. V-band light curve during the initial stage (from $t = -13$ d to 37 d). OKU data are plotted together with the SMEI data (Hounsell et al. 2010) and those taken from IAU Circulars (Yamaoka et al. 2007a,b). Both initial rising and pre-maximum halt stages are illustrated by a schematic light curve for nova eruptions (McLaughlin 1960). Peak fluctuations are observed only in the SMEI data. Dates corresponding to figures shown in this paper are indicated by vertical lines.

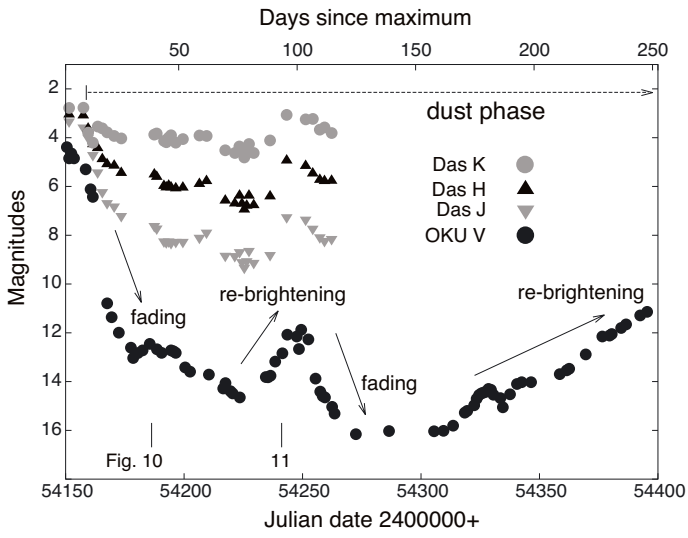

Fig. 3. V-band and JHK light curves in the post-maximum phase (dust phase). JHK data points are quoted from Das et al. (2008). There are two episodes of fading and re-brightening. Dates corresponding to figures shown in this paper are indicated by vertical lines.

layer obscuring the continuum radiation becoming partially optically thin as the dust shells expand and spread out. Hereafter, we refer to the epoch from $t = 11$ d to 250 d as the "dust phase".

From 2008 to 2011 (from $t = 420$ d to 1500 d), the magnitudes of V and y remained virtually at the same values ($y \sim 10.5$ mag) suggesting that fluxes in the optical band were contributed mainly from the photosphere and/or free-free radiation field. On the other hand, the J, H, and K_s fluxes all gradually faded to eighth magnitude in August 2010, suggesting that the NIR radiation generated by dust particles was low in 2010. V1280 Sco maintained its brightness until the final observation at OKU in April 2011 ($t = 1515$ d), displaying an exceptionally long plateau spanning over 1000 days. We guess that the continuous H-burning is the primary source of the energy emitted in the optical continuum, probably because the amount of hydrogen gas accreted onto the WD is sufficiently large to provide the fuel to be burned for a long time as suggested by Hachisu & Kato (2006) for slow novae.

Strope et al. (2010) defined seven classes of light curves among classical novae based on their shapes: the S (smooth), P (plateau), D (dust dips), C (cusps), O (oscillations), F (flat-topped), and J (jitters) classes. V1280 Sco has a combination of D- and P-class features, although neither of these characteristics in V1280 Sco is quite prototypical when compared to the original classification. A typical D-class light curve shows a deep dip caused by the dust formation around 100 days after the maximum light, whereas the dust dip of V1280 Sco appears much earlier (∼15−20 days after maximum light). In addition, V1280 Sco exhibits a re-brightening over two magnitudes during the dust dip period. Historically, no D-class nova had previously shown such a phenomenon. A typical P-class nova is defined to show a smooth, gradual decline in its optical light curve, then a long-lasting plateau phase, followed by a steep decline to the end. According to Strope et al. (2010), there is no nova that has a plateau spanning over 1000 days, with the unique exception of V1229 Aql, which followed a slanted plateau with a power-law index of −0.9, in sharp contrast to V1280 Sco (almost flat). Furthermore, none of any of the other five classifications (S, C, O, F, or J classifications) adequately describes the light curve of V1280 Sco. In the light of these findings, V1280 Sco should be considered as having a very rare light curve. The unique light curve of V1280 Sco could provide theorists with a means of deciding which parameters (the WD mass, the WD magnetic field strength, the composition of the WD envelope, and the accretion rate) determine the diverse range of features seen in light curves of novae.

4. Spectral evolution

4.1. Initial rising phase

The first spectrum taken at NHAO on 2007 February 5 ($t = -10.3$ d), only one day after the discovery, is shown in Fig. 4. It displays a smooth continuum with H I, Fe II (42)[3], Fe II (49), and Si II lines in emission, accompanied in all cases by P Cygni absorption. The absorption lines of O I and N I can also be identified. Observationally, V1280 Sco is a rare case for which a pre-maximum spectrum was obtained as early as 10 d before the maximum light. No pre-maximum spectrum had been reported in a catalog of spectroscopic observations for 27 novae (Williams et al. 2003). It may be a natural consequence of the very short (less than five days) rising time of classical novae (Warner 2008). There are several exceptional cases (V723 Cas, HR Del, V5558 Sgr, V2540 Oph, and T Pyx)[4] for which spectroscopic observations had been reported 30 days before the maximum light or earlier. Kato & Hachisu (2011) proposed a model to account for these slow novae, in which they suggested an evolution without optically thick winds. V1280 Sco might be a transitional case between typical classical novae that have a very rapid rising time and slow novae such as V723 Cas. Thanks to our spectroscopic data obtained on February 5, we can conclude that a wind flowed from the photosphere during the earliest phase of its evolution.

[3] The multiplet number is based on Moore (1959).

[4] See Iijima et al. (1998) for V723 Cas; Antipova (1978) for HR Del, Tanaka et al. (2011a) for V5558 Sgr, Tanaka et al. (2011b) for V2540 Oph, and Shore et al. (2011) for T Pyx, respectively.

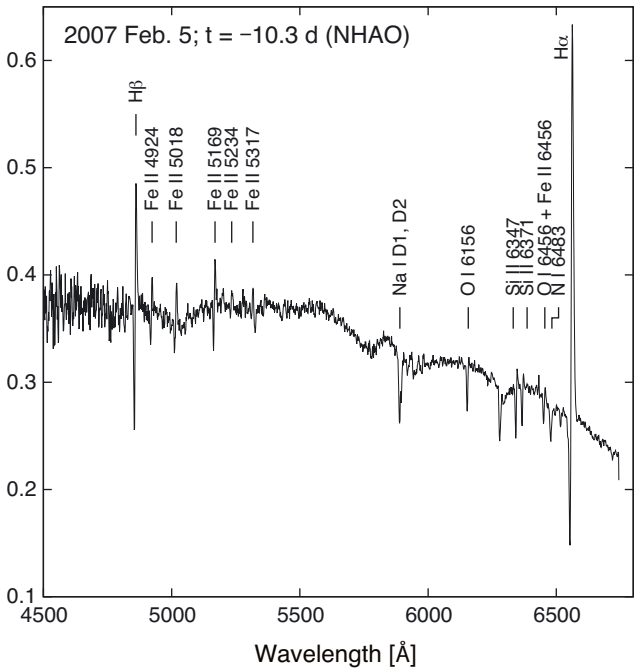

Fig. 4. A spectrum of V1280 Sco on 2007 February 5. Flux calibration has not been applied.

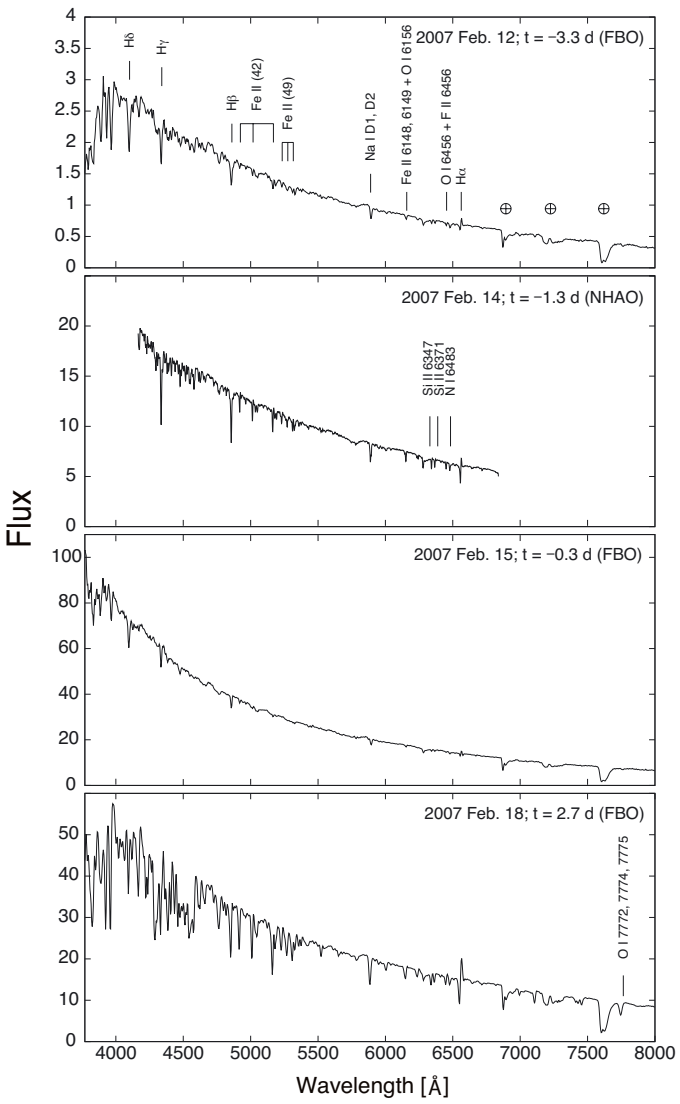

Fig. 5. Spectra of V1280 Sco from 2007 February 12 to 18. The unit of the ordinate is 10^{-11} erg cm^{-2} s^{-1} Å^{-1}.

4.2. Pre-maximum and the maximum phase

The flux in the optical region during the period between 2007 February 12 and 18 (from $t = -3.3$ d to 2.7 d) was mainly produced by the continuum radiation coming from the photosphere, and this period is referred to as the fireball phase (e.g. Shore 2008). Figure 5 shows four spectra obtained from February 12 to 18 , where the spectrum on 2007 February 12 corresponds to the pre-maximum halt stage and those obtained on 2007 February 15 and 18 correspond to the phase of peak fluctuations.

On 2007 February 12 ($t = -3.3$ d), a very weak emission component of Hα was detected, while all other emission lines were overwhelmed by the photospheric radiation to become absorption lines. On 2007 February 14 ($t = -1.3$ d), the spectrum apparently became that of an early A-type supergiant, showing weak absorption lines of He I 4472 and 5876. On 2007 February 15 ($t = -0.3$ d), close to the maximum light, the effective temperature of the photosphere became the highest because the gradient of the continuum in the blue-visual region was at its steepest. After February 15, the slope of the photospheric spectrum became less steep and the emission line of Hα became strong on 2007 February 18 ($t = 2.7$ d). At the same time, the metallic absorption lines became much deeper than in the spectrum on 2007 February 15, especially the O I 7772, 7774, and 7775 lines. The color index $B - V$ measured on February 15 at OKU was 0.39 ± 0.09. When an interstellar correction of $E(B-V) = 0.4$ was applied, the intrinsic color was $(B-V)_0 = 0.0 \pm 0.1$, corresponding to that of an early A type star.

The radial velocities measured from the blue-shifted absorption components reached their smallest values (from −100 to −300 km s^{-1}) on 2007 February 14, and their velocities then became larger after the maximum light. The observed changes in the radial velocities for various elements are displayed in Fig. 6. Similar time variations in the measured radial velocities had been found in other classical novae (e.g. Cassatella et al. 2004; Munari et al. 2008). There was an apparent trend for O I and Si II to have smaller velocities than those of Balmer and Fe II lines; the mean velocities of the Hα, Fe II, O I, and Si II lines are 620 ± 230 km s^{-1}, 510 ± 150 km s^{-1}, 320 ± 130 km s^{-1}, and 380 ± 100 km s^{-1}, respectively. Głębocki (1970) found a similar trend among the Balmer, Ca II and Fe II lines in the slow nova HR Del. He concluded that the differences in the radial velocity originate from the different lines being formed at different heights in the expanding envelope, in which a gradient in the velocity existed. For example, strong Balmer lines were formed in a layer further from the central ignition region than the forming region of the weaker lines of ionized metals. Consequently, the expansion velocity in the part of the envelope where absorption lines were formed was increasing (accelerating) with height.

Figure 7 shows the spectrum obtained at NHAO on 2007 February 19 ($t = 3.7$ d). It displays a typical spectral feature of Fe II type novae around the maximum light. The continuum spectrum weakened and emission lines of Hβ, O I, Fe II, and Si II became strong, exhibiting P Cygni profiles. On the night of February 19, the Na I D1 and D2 lines appeared in emission for the first time.

As shown in Fig. 8, the photospheric component significantly weakened and the continuum was flat on

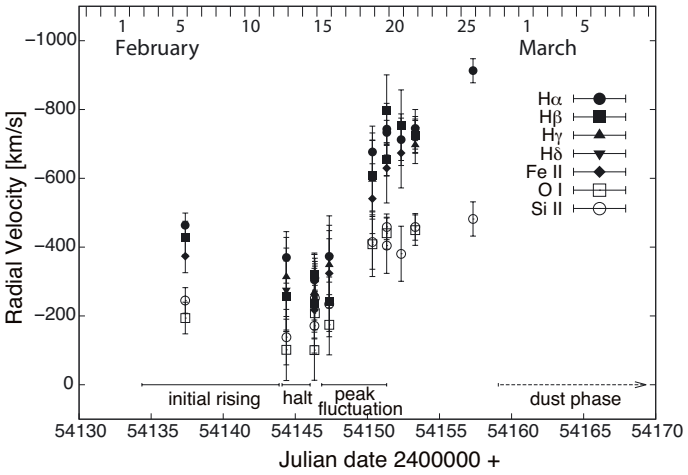

Fig. 6. Radial velocities of absorption components.

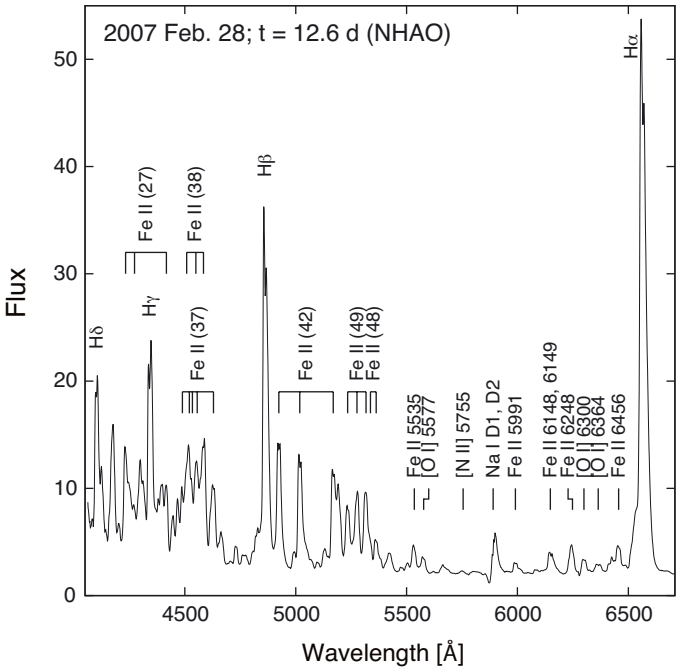

Fig. 9. A spectrum of V1280 Sco on 2007 February 28. The unit of the ordinate is 10^{-11} erg cm^{-2} s^{-1} Å^{-1}.

2007 February 21 (t = 5.6 d). This means that the free-free radiation contributed significantly to the continuum flux as the photosphere shrunk and the region of optically thin gas extended at the same time. The absorption components became weaker, especially as the minimum point of the Hα absorption reached the local continuum level.

4.3. Dust phase

The forbidden lines of [O I] 5577 and [O I] 6300, 6364 were first observed on 2007 February 28 (t = 12.6 d) in our observations (Fig. 9). The shape of permitted lines such as H I and Fe II changed into a double-peaked structure. The strengths of the double peaks in each of the Balmer lines were different; the blue components were stronger than the red components in Hα and Hβ, while the blue components were weaker in Hγ and Hδ.

Figure 10 shows a tracing of a spectrum obtained at NHAO on 2007 March 25 (t = 37.6 d). In the spectrum, Hβ weakened

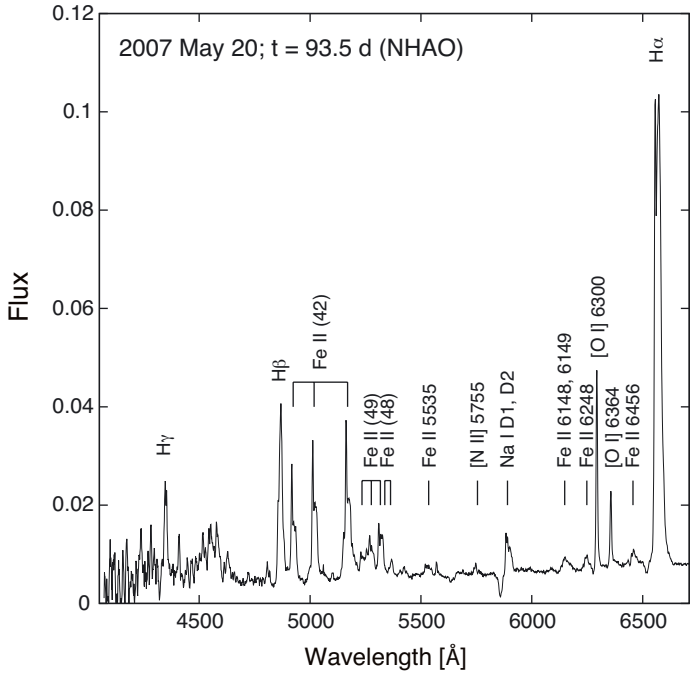

Fig. 11. A spectrum of V1280 Sco on 2007 May 20. The unit of the ordinate is 10^{-11} erg cm^{-2} s^{-1} Å^{-1}.

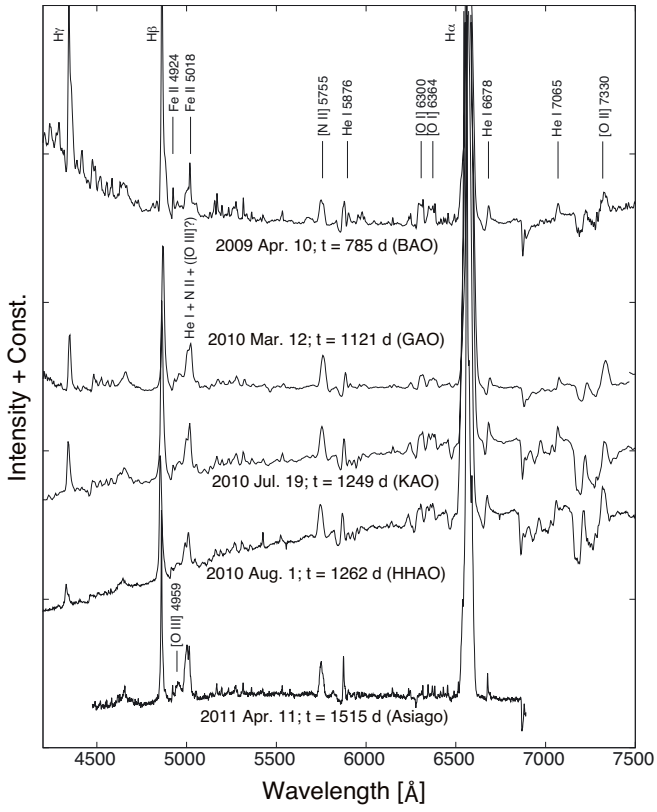

Fig. 13. Spectra of V1280 Sco from 2009 to 2011.

significantly and its strength was comparable to those of the Fe II (42) lines. Furthermore, the double-peaked structure of Hα had changed dramatically between 2007 February 28 and March 25. Its red peak was stronger on March 25, reversing the V/R ratio within ~25 days.

When the decline in the brightness in the optical band began owing to the dust formation from March to mid-May 2007, the continuum flux was too weak to be detected by our instruments and the Hβ, Hγ, and Hδ emission lines also remained undetected. However, during the re-brightening phase (from t = 85 d to 110 d), we succeeded in obtaining a spectrum with high signal-to-noise ratio in the continuum. Figure 11 shows a spectrum obtained at NHAO on 2007 May 20 (t = 93.5 d), which was the first one acquired after the dust formation event had initiated. In the May 20 spectrum, Hβ and Hγ lines had reappeared. On the same spectrum, the Hα line exhibited a double-peaked structure accompanied by a P Cygni absorption feature extending up to 2000 km s^{-1} in velocity. The red peak of the double-peaked Hα emission became much broader ($FWHM$ ~ 1200 km s^{-1}). These might be connected with the second large outflow triggered by a new burst on the surface of the WD in the re-brightening period.

4.4. Plateau from 2008 to 2010

As shown in Fig. 12, we find that He I 5876 and He I 6678 appeared in emission on 2008 September 9 (t = 571 d) for the first time. This indicates that the photospheric temperature was higher than that in 2007, although the temperature was not high enough to produce [O III] or He II lines. The forbidden lines of [N II] 5755 and [O I] 6300, 6364 were broader than in 2007. P Cygni absorptions appeared in both Balmer and Fe II lines, indicating that wind was outflowing due to continuous H-burning.

Figure 13 shows tracings of five spectra obtained at BAO on 2009 April 10 (t = 785 d), at GAO on 2010 March 12 (t = 1121 d), at KAO on 2010 July 19 (t = 1249 d), at HHAO on 2010 August 1 (t = 1262 d), and at Asiago on 2011 April 11 (t = 1515 d). The [O II] 7330 line could be detected owing to the wider wavelength coverage at BAO, GAO, KAO, and HHAO. Spectra during the period were dominated by the continuum flux that probably originated from the ongoing free-free radiation that lasted for more than five years. There was almost no clear spectral variation between 2009 and 2011, during which there were either appearances or disappearances of major emission lines. There is an emission line near 5010 Å from t = 785 d to 1262 d in Fig. 13. We attribute this line mainly to Fe II 5018 and He I 5016, and not to the forbidden line of [O III] 5007. This is because the weaker component [O III] 4959 was absent before t = 1262 d. However, we note that the nebular lines of [O III] 4959 and 5007 evolved very slowly; [O III] 4959 was detected in a spectrum taken at Asiago on 2011 April 11. The transitional period to the nebular phase is reported in detail in Sect. 4.5. Both the He I 5876 and 6678 lines were observed with P Cygni absorption indicating that the wind persisted until April 2011.

4.5. Onset of the nebular phase in 2011

High resolution spectra from 4800 Å to 5050 Å obtained with the Subaru telescope from March to July 2011 are displayed in Fig. 14. This figure shows that the nebular lines of [O III] 4959 and 5007 were definitely establishing themselves during this period. To compare with the slow nova V723 Cas, we followed a definition of the onset of the nebular phase noted in Iijima (2006), in which *both* of the [O III] 4959 and 5007 lines must be identified definitely. We therefore conclude that V1280 Sco had entered the nebular phase between March and April 2011, more than 1500 d (50 months) after the maximum light. This means that it took a very long time for the photosphere to shrink so as to become hotter and emit enough ultraviolet radiation to excite doubly ionized oxygen atoms into the second energy level of 35.1 eV. However, even hotter radiation field is needed to produce He II lines for which an energy of 54.4 eV is needed. We detected no trace of the He II 4686 line in a spectrum obtained on 2011 July 24 with the Subaru telescope. Since the historically longest transitional time to enter the nebular phase of about 18 months was observed in V723 Cas (Iijima 2006), we conclude that V1280 Sco is going through the slowest spectral evolution ever observed for known classical novae.

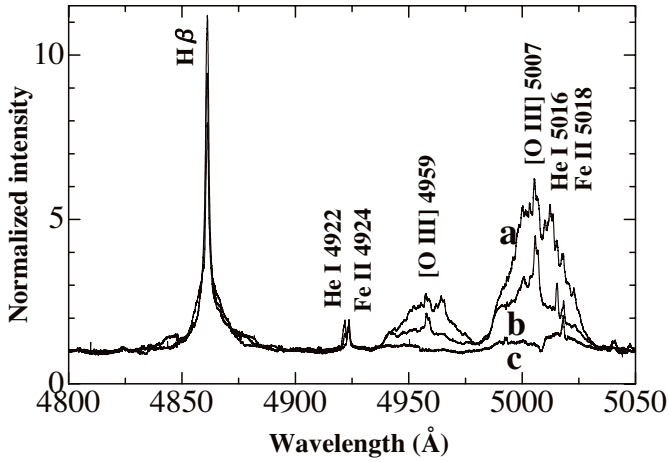

Fig. 14. High dispersion spectra from 4800 Å to 5050 Å observed with the Subaru telescope in 2011. Hβ and the nebular lines [O III] 4959, 5007 are displayed. Labels a, b, and c represent data obtained on July 24 (t = 1619 d), June 12 (t = 1577 d), and March 17 (t = 1490 d), respectively. The [O III] 4959 line is absent on March 17, while it can be clearly seen on June 12.

5. Discussion

5.1. Distance and mass of the WD

The distance to V1280 Sco was estimated to be 1.6 ± 0.4 kpc and 630 ± 100 pc by Chesneau et al. (2008) and Hounsell et al. (2010), respectively. The substantial difference in these results is caused mainly by the difficulty in measuring the velocities of both the dust shells and photosphere. Chesneau et al. (2008) estimated the distance by comparing the apparent size of the dust shell obtained from direct observations to the calculated size, where they assumed an expansion velocity of 500 ± 100 km s^{-1}. However, it is difficult to measure the velocity of the dust shells reliably because the wind speed was variable before the dust phase as shown in Sect. 4.2 (Fig. 6). When we assume that the velocity of the dust shell is 350 ± 160 km s^{-1}, which is the mean velocity measured from the blue-shifted absorption lines of O I and Si II, the distance is estimated to be d = 1.1 ± 0.5 kpc by adopting the apparent size of the dust shell reported in Chesneau et al. (2008).

We next attempt to evaluate the mass of the WD by using the observed pre-maximum halt shown in Fig. 2. Hachisu & Kato (2004) showed that the brightness of a nova at the pre-maximum halt is determined by its Eddington luminosity; it is governed primarily by the mass of a WD ($M_{\rm WD}$), and is a good candidate as a standard candle. The absolute magnitude during the pre-maximum halt is expressed by the relation

$$M_{\rm V,\ halt} \approx -1.53(M_{\rm WD}/M_{\odot}) - 4.26 \quad (1)$$

for the solar composition in WD envelopes, where $M_{\rm V,\ halt}$ is the absolute magnitude at the pre-maximum in V-band. They also showed that the absolute magnitude of the pre-maximum halt depends slightly on the composition of the WD envelopes. A relation for the case $X = 0.35$, $Y = 0.33$, and $Z = 0.32$ (C+O = 0.30) is given as

$$M_{\rm V,\ halt} \approx -1.75(M_{\rm WD}/M_{\odot}) - 4.25. \quad (2)$$

These relations are valid for classical novae exhibiting a pre-maximum halt in the mass range of $0.6 \leq M_{\rm WD}/M_{\odot} \leq 1.3$. A comparison of Eqs. (1) and (2) shows that the variation in $M_{\rm V,\ halt}$ when the composition changes from solar abundances to enrichments of C + O = 0.30 is at most about ten percent. When we use our observational results (the magnitude at the pre-maximum halt period of $m_{\rm V,\ halt} = 6.3$ and the interstellar extinction $A_{\rm v} = 1.2$) in Eqs. (1) and (2) using the distance $d = 1.1$ kpc, we obtain the mass of the WD of 0.6 $M_{\odot}$ from Eq. (1) and an even lower value in Eq. (2). To determine the WD mass more accurately, further analyses including other parameters (the abundances of He and CNO in WD envelopes, the WD magnetic field strength, etc.) and/or extending the range of WD mass in the theory are needed. In any case, we infer that the mass of a WD in V1280 Sco is most likely to be ~0.6 $M_{\odot}$ or lower, which is consistent with being a very slow nova as our observations show.

5.2. Mass in the shell

We estimate the mass of the nova ejecta using [O I] lines at $\lambda\lambda$5577, 6300, and 6364 for two cases: (1) the solar abundance of oxygen ([O/H] = 0.0) and (2) an over-abundance of oxygen ([O/H] = +1.0). The latter case is motivated by the observational trend that dust-forming novae have enrichments of CNO elements (Gehrz 1988, and references therein). These [O I] lines are used to estimate the physical parameters and the mass contained in the shell for classical novae, which was first described in Williams (1994). The optical depth (τ) of the λ6300 line can be obtained from the flux ratio of $F_{\lambda 6300}$ to $F_{\lambda 6364}$ as

$$\frac{F_{\lambda 6300}}{F_{\lambda 6364}} = \frac{(1 - {\rm e}^{-\tau})}{(1 - {\rm e}^{-\tau/3})}, \quad (3)$$

where the ratio approaches three and one when the optical depth approaches zero and a moderately large value, respectively. For the observed ratio of $F_{\lambda 6300}$ to $F_{\lambda 6364} = 1.3$, we find that the value of τ is 4.1 on 2007 February 28, which represents the largest optical depth before the inner part of the expanding envelope is obscured by dust. This value is in good agreement with the result of Kucnarayakti et al. (2008). The electron temperature ($T_{\rm e}$) can be derived through the formula of Williams (1994)

$$T_{\rm e} = \frac{11\,200}{\log[43\tau/(1 - {\rm e}^{-\tau}) \times F_{\lambda 6300}/F_{\lambda 5577}]}\ {\rm K}. \quad (4)$$

With the optical depth and the electron temperature determined by using Eqs. (3) and (4), we can estimate the mass of neutral oxygen ($M_{\rm O\,I}$) contained in the ejecta from the relation

$$M_{\rm O\,I} = 152\, {d_{\rm kpc}}^2 \exp\left(\frac{22850}{T_{\rm e}}\right) \times \frac{\tau}{(1 - {\rm e}^{-\tau})} F_{\lambda 6300}\, M_{\odot}, \quad (5)$$

where $d_{\rm kpc}$ is the distance to the object in kpc. The equation is slightly modified from the original one given in Williams (1994) to apply to spectra already corrected for interstellar extinction.

Table 4. Physical parameters.

Date	τ	$T_{\rm e}$(K)	$M_{\rm O\,I}$ ($M_{\odot}$)	$M_{\rm ejecta}$ ($M_{\odot}$)	
				[O/H] = 0.0	[O/H] = +1.0
2007					
Feb. 28	4.10	5500	1.4×10^{-5}	2.3×10^{-3}	2.3×10^{-4}
Mar. 7	0.37	5400	5.2×10^{-7}	9.1×10^{-5}	9.1×10^{-6}
Mar. 21	0.15	5000	2.0×10^{-7}	3.4×10^{-5}	3.4×10^{-6}
Mar. 25	0.17	5200	2.3×10^{-7}	3.9×10^{-5}	3.9×10^{-6}
Apr. 11	0.48	4400	3.8×10^{-7}	6.6×10^{-5}	6.6×10^{-6}

The derived physical parameters from 2007 February 28 to April 11 are listed in Table 4. The results of the line flux measurements for [O I] lines, together with other major absorption and emission lines, are listed in Table 5. From 2007 Feb. 28 to Apr. 11, all oxygen atoms in the V1280 Sco ejecta can be assumed to have been in the neutral state because no [O II] line was observed in 2007 observations, hence the mass derived for neutral oxygen corresponds to the total mass of oxygen in the ejecta ($M_{\rm O} = M_{\rm O\,I}$). Adopting the solar chemical abundance of Asplund et al. (2009), we can estimate the total ejected mass ($M_{\rm ejecta}$) in the first eruption to be on the order of 10^{-3}–10^{-4} $M_{\odot}$, which depends on the assumed abundance of oxygen. The higher mass corresponds to the case of the solar abundance of oxygen and the lower one to the overabundance of oxygen.

In both cases, these results strengthen our view that V1280 Sco belongs to the class of slow novae, which tend to have more massive ejecta than ordinary novae (10^{-5}–10^{-6} $M_{\odot}$). After March 7 (dust phase), the values of $M_{\rm ejecta}$ become much lower than on February 28. The apparent decline seems to be due to an obscuration of the emitting region of the [O I] lines by the thick dust shells.

6. Summary

Our observations have revealed that V1280 Sco is an extremely slowly evolving nova. This claim is based on the following findings:

1. V1280 Sco declined in brightness gradually at a very slow rate from its discovery to our last photometric observation in 2011.
2. It has a very long plateau spanning over 1000 days in its light curve.
3. It takes a very long time (~50 months after the burst) to enter the nebular phase.
4. The wind is ongoing at least for about 1500 days until 2011.

Among the known slow novae, V723 Cas had spent about 18 months before entering the nebular phase (Iijima 2006) and GQ Mus had the H-burning turn-off time of about 3000 days from which Hachisu et al. (2008) estimated the wind-off time of 1000 days. V1280 Sco has spent about three times longer than V723 Cas to enter the nebular phase and has exceeded the previous record of the wind-off time of GQ Mus. According to Kato & Hachisu (1994), the timescale of nova evolution is strongly correlated with the WD mass, so that the observations of V1280 Sco suggest that its burst occurred at a very low mass WD comparable to 0.7 $M_{\odot}$ of GQ Mus (Hachisu et al. 2008) or 0.59 $M_{\odot}$ of V723 Cas (Hachisu & Kato 2004) or even lower. However, because the timescale is also slightly depends on the abundances, further analyses including the effect of the abundance of V1280 Sco and/or other parameters should be carried out by theorists.

The distance is estimated to be 1.1 ± 0.5 kpc, based on measurements of the velocities of the expanding shell and direct measurements of the apparent size. When we take the observed magnitude at the pre-maximum halt stage into account, the distance corresponds to the WD mass of ~0.6 $M_\odot$ or lower (Hachisu & Kato 2004). Adopting the distance of 1.1 kpc, we estimated the mass in the initial ejecta to be on the order of 10^{-3}–10^{-4} $M_\odot$ from the [O I] line analysis. The dust formation occurred at a very early phase, which might have been connected to the far larger amount of ejected material than for ordinary novae (10^{-5}–10^{-6} $M_\odot$).

Acknowledgements. We are grateful to the Nishi-Harima Astronomical Observatory staff and KANATA team for their supports during observations. We gratefully acknowledge the cooperation of students at Osaka Kyoiku University who helped us to perform the photometric observations. We would like to thank Masaki Nagamori and Yukio Ueno, who aided our spectroscopic observations at Bisei Astronomical Observatory. We sincerely thank Izumi Hachisu and Mariko Kato for useful comments. Thanks are also due to Kuzunori Ishibashi and Shinjirou Kouzuma for their careful reading of the manuscript and suggestions. This work was supported by the Global COE Program of Nagoya University "Quest for Fundamental Principles in the Universe (QFPU)" from JSPS and MEXT of Japan. M.Y. has been supported by the JSPS Research Fellowship for Young Scientists.

References

Antipova, L. I. 1978, SvA, 22, 306
Asplund, M., Grevesse, N., Sauval, A. J., & Scott, P. 2009, ARA&A, 47, 481
Bode, M. F., & Evans, A. 2008, Classical Novae (Cambridge: Cambridge Univ. Press)
Cassatella, A., Lamers, H. J. G. L. M., Rossi, C., et al. 2004, A&A, 420, 571
Chesneau, O., Banerjee, D. P. K., Millour, F., et al. 2008, A&A, 487, 223
Chochol, D., Katysheva, N. A., Pribulla, T., et al. 2005, Contributions of the Astronomical Observatory Skalnate Pleso, 35, 107
Crawford, D. L. 1987, A short tutorial on Strömgren four-color photometry, in New generation small telescopes, ed. D. S. Hayes, R. M. Genet, & D. R. Genet, 345
Cutri, R. M., Skrutskie, M. F., van Dyk, S., et al. 2003, 2MASS All-Sky Catalog of Point Sources, Vizier online data catalog II/246
Das, R. K., Ashok, N. M., & Banerjee, D. P. K. 2007, CBET 866, 1
Das, R. K., Banerjee, D. P. K., Ashok, N. M., & Chesneau, O. 2008, MNRAS, 391, 1874
Friedjung, M. 1966, MNRAS, 132, 317
Gehrz, R. D. 1988, ARA&A, 26, 377
Głębocki, R. 1970, Acta Astron., 20, 99
Gray, R. O. 1998, AJ, 116, 482
Hachisu, I., & Kato, M. 2004, ApJ, 612, L57
Hachisu, I., & Kato, M. 2006, ApJS, 167, 59
Hachisu, I., & Kato, M. 2007, ApJ, 662, 552
Hachisu, I., Kato, M., Kiyota, S., et al. 2006, ApJ, 651, L141
Hachisu, I., Kato, M., & Cassatella, A. 2008, ApJ, 687, 1236
Henden, A., & Munari, U. 2007, IBVS, 5771, 1
Hounsell, R., Bode, M. F., Hick, P. P., et al. 2010, ApJ, 724, 480
Iijima, T. 2006, A&A, 451, 563
Iijima, T., Rosino, L., & della Valle, M. 1998, A&A, 338, 1006
Kandori, R., Kusakabe, N., Tamura, M., et al. 2006, SPIE, 6269, 159
Kato, M., & Hachisu, I. 1994, ApJ, 437, 802
Kato, M., & Hachisu, I. 2011, ApJ, 743, 157
Kawabata, K. S., Nagae, O., Chiyonobu, S., et al. 2008, SPIE, 7014, 151
Kuncarayakti, H., Kristyowati, D., & Kunjaya, C. 2008, Ap&SS, 314, 209
McLaughlin, D. B. 1960, The Spectra of Novae, in Stellar Atmospheres, ed. J. L. Greenstein (Chicago: The Univ. of Chicago Press), 585
Moore, C. E. 1959, Natl. Bur. Std. U. S. Tech. Note (Washington, D.C.: Office of Technical Services, US Department of Commerce), 36
Munari, U., Valisa, P., Dalla Via, G., & Dallaporta, S. 2007, CBET, 852, 1
Munari, U., Henden, A., Valentini, M., et al. 2008, MNRAS, 387, 344
Naito, H., & Narusawa, S. 2007, IAU Circ., 8803, 2
Noguchi, K., Aoki, W., Kawanomoto, S., et al. 2002, PASJ, 54, 855
Ozaki, S., & Tokimasa, N. 2005, Annual Report of the Nishi-Harima Astronomical Observatory, 15, 15
Sadakane, K., Tajitsu, A., Mizoguchi, S., et al. 2010, PASJ, 62, L5
Samus, N. N., Durlevich, O. V., et al. 2004, Combined General Catalogue of Variable Stars (GCVS4.2)
Shore, S. N. 2008, Optical and ultraviolet evolution, in Classical Novae, ed. M. F. Bode, & A. Evans, 2nd edn. (Cambridge: Cambridge Univ. Press), 194
Shore, S. N., Augusteijn, T., Ederoclite, A., & Uthas, H. 2011, A&A, 533, L8
Strope, R. J., Schaefer, B. E., & Henden, A. A. 2010, AJ, 140, 34
Tanaka, J., Nogami, D., Fujii, M., et al. 2011a, PASJ, 63, 159
Tanaka, J., Nogami, D., Fujii, M., et al. 2011b, PASJ, 63, 911
Warner, B. 1995, Cataclysmic Variable Stars (Cambridge: Cambridge Univ. Press)
Warner, B. 2008, Properties of novae: an overview, in Classical Novae, ed. M. F. Bode, & A. Evans, 2nd edn. (Cambridge: Cambridge Univ. Press), 16
Williams, R. E. 1992, AJ, 104, 725
Williams, R. E. 1994, ApJ, 426, 279
Williams, R. E., Hamuy, M., Phillips, M. M., et al. 2003, J. Astron. Data, 9, 3
Yamaoka, H., Nakamura, Y., Nakano, S., et al. 2007a, IAU Circ., 8803, 1
Yamaoka, H., Waagen, E., Amorim, A., et al. 2007b, IAU Circ., 8807, 1
Yamaoka, H., Fujii, M., & Naito, H. 2007c, IAU Circ., 8807, 2

Pages 11 to 16 are available in the electronic edition of the journal at http://www.aanda.org

Table 2. BVR_cI_cy magnitudes of V1280 Sco observed at OKU.

JD	Magnitudes									
2 400 000+	B (err.)		V (err.)		R_c (err.)		I_c (err.)		y (err.)	
54144			6.26	0.08					6.44	0.08
54146			5.27	0.07	5.04	0.06	4.76	0.05	5.30	0.07
54147	4.57	0.05	4.18	0.08	4.04	0.07	3.81	0.05	4.29	0.07
54148			4.58	0.09	4.38	0.09				
54150	4.94	0.05	4.39	0.07	4.05	0.07	3.75	0.31	4.39	0.07
54151			4.85	0.07	4.37	0.07			4.91	0.07
54152	5.39	0.06	4.65	0.15	4.15	0.06	3.84	0.06	4.75	0.07
54153	5.45	0.05	4.85	0.07	4.32	0.06			4.96	0.07
54158	5.66	0.05	5.30	0.07	4.70	0.06	4.27	0.05	5.56	0.07
54160	6.42	0.06	6.12	0.07	5.38	0.06			6.53	0.07
54161	6.74	0.05	6.43	0.07	5.67	0.12			6.91	0.07
54167	11.12	0.05	10.80	0.07	9.77	0.06	9.26	0.04	11.42	0.07
54169	11.76	0.09	11.36	0.07	10.30	0.06			12.03	0.08
54172			11.99	0.08	10.88	0.08				
54177			12.61	0.08	11.50	0.06	11.02	0.04	13.45	0.18
54178			13.03	0.11	11.59	0.08	11.14	0.04		
54180			12.83	0.07	11.75	0.06	11.38	0.04	13.58	0.09
54181			12.30	0.35	11.51	0.08	10.97	0.04		
54182			12.72	0.09	11.67	0.06	11.13	0.04		
54185			12.45	0.07	11.36	0.06	10.82	0.04	13.14	0.11
54188			12.68	0.07	11.60	0.06	11.25	0.04	13.41	0.22
54190			12.82	0.07	11.72	0.06	11.58	0.04	13.53	0.09
54194			12.73	0.07	11.60	0.06	11.48	0.04	13.56	0.14
54195			12.76	0.09	11.61	0.06	11.47	0.05	13.47	0.16
54196			12.82	0.09	11.66	0.07	11.43	0.05	13.85	0.27
54200			13.43	0.10	12.34	0.06	11.87	0.05		
54202			13.59	0.12	12.37	0.06	11.68	0.05	14.21	0.22
54210			13.71	0.09	12.59	0.06	11.85	0.06		
54216			14.28	0.13	13.24	0.07	12.67	0.05		
54217			14.06	0.17	13.16	0.12	12.64	0.12		
54219			14.40	0.11	13.34	0.06	12.65	0.04		
54220			14.48	0.16	13.34	0.10	12.66	0.06	14.82	0.23
54223			14.65	0.17	13.14	0.21				
54234			13.82	0.24	12.70	0.11	11.95	0.07		
54235			13.83	0.13	12.87	0.06	12.00	0.05	14.26	0.17
54236			13.76	0.13	12.76	0.07	11.97	0.05	14.18	0.12
54238			13.18	0.08	12.13	0.06	11.23	0.04	13.58	0.10
54241			12.84	0.07	11.76	0.06	10.89	0.04	13.28	0.08
54243			12.08	0.07					12.46	0.10
54247	13.12	0.11	12.15	0.08	11.11	0.06	10.35	0.05	12.56	0.10
54248	13.31	0.06	12.67	0.21	11.48	0.31	10.67	0.05	12.89	0.08
54249	12.84	0.07	11.87	0.08	10.82	0.07	10.13	0.30	12.21	0.09
54252			12.27	0.14	11.31	0.07	10.68	0.19	12.84	0.21
54255			13.88	0.14	12.75	0.07	12.08	0.04	14.64	0.17
54257			14.41	0.15	13.19	0.09	12.40	0.13	15.08	0.17
54258			14.60	0.17	13.30	0.07	12.31	0.09	15.75	0.17
54259			14.66	0.14	13.34	0.07	12.30	0.05	15.33	0.17
54262			15.03	0.09	13.80	0.06	12.67	0.11	15.67	0.17
54263			15.31	0.15	14.16	0.09	13.17	0.05	16.16	0.17
54272			16.15	0.17	14.42	0.16	14.45	0.16		
54286			16.03	0.17	14.88	0.16	14.94	0.16		
54305			16.04	0.10	15.06	0.06	14.90	0.05		
54309			16.02	0.18	15.05	0.09	14.71	0.08		
54313			15.80	0.14	14.87	0.08	14.49	0.07		
54318			15.28	0.27	14.36	0.20	13.82	0.06		
54319			15.21	0.12	14.31	0.08	13.83	0.08		
54322			14.97	0.09	13.93	0.07	13.42	0.04	15.49	0.19
54323			14.71	0.08	13.66	0.08	13.14	0.05		
54324			14.55	0.16	13.56	0.12				
54325			14.49	0.08	13.50	0.06				
54326			14.45	0.11	13.49	0.07	12.93	0.04		
54327			14.41	0.09	13.42	0.06	12.78	0.04		
54328			14.30	0.11	13.28	0.07	12.71	0.04		
54329			14.33	0.09	13.32	0.07	12.70	0.05		
54330			14.55	0.08	13.49	0.06	12.87	0.05		
54333			14.68	0.13	13.58	0.07	13.09	0.05		
54334			15.06	0.17	13.71	0.09	13.15	0.06		

Table 2. continued.

JD	Magnitudes									
2 400 000+	B (err.)		V (err.)		R_c (err.)		I_c (err.)		y (err.)	
54337			14.52	0.10	13.38	0.06	12.81	0.06		
54340			14.10	0.11	13.08	0.09	12.52	0.07		
54342			14.02	0.08	12.90	0.06	12.30	0.04	14.32	0.19
54346			14.03	0.08	12.89	0.06	12.28	0.04		
54358			13.70	0.11	12.61	0.07	12.11	0.06		
54361			13.54	0.08	12.46	0.06	11.91	0.04	14.00	0.14
54362			13.47	0.08	12.36	0.06	11.85	0.04	13.91	0.09
54369	13.67	0.15	12.90	0.08	11.86	0.06	11.42	0.05	13.05	0.13
54376	12.80	0.10	12.16	0.07	11.41	0.06	10.98	0.04		
54379			12.11	0.08	11.23	0.06	10.81	0.04	12.30	0.22
54380			12.05	0.07	11.18	0.07	10.76	0.04	12.18	0.08
54384			11.81	0.07	10.91	0.06	10.44	0.06	11.89	0.08
54386	12.77	0.14	11.65	0.21	11.06	0.31	10.42	0.04	11.99	0.08
54392			11.29	0.27	10.82	0.15	10.28	0.15		
54395			11.14	0.16	10.37	0.16	10.06	0.07		
54490			11.27	0.10	10.55	0.08	9.99	0.09		
54491	11.93	0.07	11.09	0.10	10.28	0.06	9.74	0.10		
54503	11.73	0.37	11.17	0.08	10.49	0.07	9.97	0.04		
54536	12.06	0.11	11.37	0.07	10.99	0.08	10.07	0.06		
54543	12.04	0.08	11.26	0.07	10.64	0.07	10.01	0.05		
54561	11.71	0.07	10.94	0.07	10.18	0.06	9.88	0.05	11.08	0.07
54571	11.56	0.05	10.87	0.07	10.12	0.06	9.82	0.05	11.01	0.07
54578	11.45	0.05	10.68	0.08	9.99	0.07	9.71	0.06	10.81	0.08
54585	11.31	0.06	10.53	0.08	9.89	0.07	9.57	0.04	10.70	0.07
54593	11.34	0.05	10.58	0.07	9.95	0.06	9.65	0.05	10.74	0.07
54601	11.37	0.05	10.62	0.08	9.96	0.06	9.68	0.04	10.76	0.07
54613	11.14	0.05	10.42	0.08	9.77	0.07	9.48	0.05	10.54	0.07
54627	11.01	0.05	10.31	0.07	9.74	0.07	9.45	0.05	10.53	0.07
54631	11.00	0.05	10.33	0.07	9.71	0.06	9.42	0.05	10.48	0.07
54642	10.95	0.05	10.29	0.07	9.71	0.08	9.39	0.05	10.45	0.08
54652	10.94	0.05	10.27	0.07	9.68	0.06	9.42	0.08	10.45	0.07
54658	10.90	0.05	10.24	0.07	9.64	0.06	9.32	0.04	10.38	0.07
54674	10.87	0.05	10.23	0.07	9.62	0.07	9.34	0.05	10.37	0.07
54689	10.80	0.05	10.17	0.10	9.61	0.07	9.30	0.08	10.33	0.07
54692	10.71	0.05	10.08	0.07	9.53	0.07	9.23	0.05	10.24	0.07
54699	10.74	0.06	10.14	0.07	9.51	0.06			10.28	0.08
54703	10.70	0.07	10.07	0.09	9.47	0.07	9.25	0.05	10.21	0.08
54718	10.65	0.07	10.05	0.09	9.37	0.06	9.19	0.04	10.14	0.07
54726	10.65	0.05	10.08	0.08	9.45	0.13	9.24	0.05	10.17	0.07
54732	10.57	0.05	10.06	0.09	9.37	0.08	9.24	0.04	10.22	0.09
54734	10.48	0.39	9.94	0.28	9.43	0.06	9.20	0.11	10.13	0.13
54741	10.59	0.05	10.00	0.07	9.37	0.08	9.14	0.07	10.08	0.07
54748	10.60	0.05							10.15	0.12
54872	10.48	0.06	9.86	0.07	9.34	0.06	9.04	0.04	10.01	0.07
54881	10.55	0.06	10.01	0.07	9.37	0.07	9.09	0.04	10.10	0.07
54903	10.66	0.05	10.07	0.07	9.45	0.06	9.15	0.04	10.15	0.07
54929	10.86	0.06	10.22	0.08	9.46	0.07	9.28	0.04	10.37	0.07
54946	10.91	0.06	10.28	0.07	9.56	0.06	9.26	0.05	10.37	0.07
54953			10.27	0.07	9.61	0.06	9.29	0.04	10.39	0.08
54961	10.95	0.06	10.29	0.08	9.66	0.07	9.36	0.05	10.44	0.07
54978	10.95	0.05	10.30	0.07	9.61	0.06	9.33	0.04	10.45	0.07
55069	11.60	0.05	10.92	0.07	10.16	0.07	9.84	0.04	11.08	0.07
55268	11.22	0.12	10.60	0.07	9.94	0.06	9.54	0.05	10.73	0.07
55293	11.26	0.06	10.57	0.07	9.84	0.06	9.54	0.04	10.73	0.08
55317									10.69	0.07
55319			10.48	0.07	9.74	0.06	9.44	0.05	10.62	0.07
55322	11.13	0.06	10.47	0.08	9.75	0.07	9.44	0.05	10.63	0.08
55358	11.12	0.05	10.49	0.08	9.80	0.07	9.48	0.04	10.63	0.07
55399			10.36	0.07	9.66	0.07	9.36	0.05	10.47	0.08
55402	11.07	0.06	10.45	0.08	9.73	0.07	9.48	0.05	10.57	0.07
55411	10.90	0.07	10.32	0.09	9.65	0.06	9.34	0.05	10.45	0.08
55414	11.03	0.05	10.37	0.07	9.66	0.07	9.35	0.05	10.50	0.07
55426	11.11	0.05	10.46	0.08	9.73	0.06	9.46	0.05	10.60	0.07
55449	11.16	0.05	10.53	0.08	9.81	0.06	9.50	0.05	10.69	0.07
55657	11.05	0.05	10.46	0.07	9.80	0.06	9.60	0.04		
55663									10.65	0.07

Table 3. Journal of spectroscopic observations of V1280 Sco.

Date UT	JD 2 400 000+	Range Å	Resolution Å	Exp. s	Observatory	Phase	Remarks
2007							
Feb. 5.87	54 137.37	4100-6760	4.7	900	NHAO	initial rising	Fig. 4†
Feb. 12.88	54 144.38	3750-8250	10	540	FBO	pre-maximum halt	Fig. 5
Feb. 14.83	54 146.33	3750-8250	10	900	FBO	pre-maximum rising	
Feb. 14.86	54 146.36	4160-6820	4.7	600	NHAO	pre-maximum rising	Fig. 5
Feb. 15.86	54 147.36	3750-8250	10	1380	FBO	peak fluctuations	Fig. 5
Feb. 16.80	54 148.30	4160-6820	4.7	600	NHAO	peak fluctuations	†
Feb. 18.85	54 150.35	3750-8250	10	600	FBO	peak fluctuations	Fig. 5
Feb. 19.84	54 151.34	4160-6820	4.7	300	NHAO		Fig. 7∗
Feb. 19.84	54 151.34	3750-8250	10	1000	FBO		
Feb. 20.84	54 152.34	3750-8250	10	470	FBO		
Feb. 21.82	54 153.32	4160-6820	4.7	600	NHAO		Fig. 8∗
Feb. 25.83	54 157.33	4160-6820	4.7	300	NHAO		
Feb. 25.86	54 157.36	3750-8250	10	144	FBO		
Feb. 27.84	54 159.34	3750-8250	10	120	FBO	dust phase	
Feb. 28.81	54 160.31	4160-6820	4.7	300	NHAO	dust phase	Fig. 9
Mar. 6.85	54 166.35	3750-8250	10	1440	FBO	dust phase	
Mar. 7.80	54 167.30	4160-6820	4.7	1800	NHAO	dust phase	
Mar. 8.85	54 168.35	3750-8250	10	1440	FBO	dust phase	
Mar. 16.82	54 176.32	3750-8250	10	1800	FBO	dust phase	
Mar. 21.82	54 181.32	4160-6820	4.7	1800	NHAO	dust phase	
Mar. 25.80	54 185.30	4160-6820	4.7	2400	NHAO	dust phase	Fig. 10∗
Apr. 11.82	54 202.32	4160-6820	4.7	2400	NHAO	dust phase	
May 2.78	54 223.28	4160-6820	4.7	4800	NHAO	dust phase	
May 7.74	54 228.24	4160-6820	4.7	5400	NHAO	dust phase	
May 20.69	54 241.19	4160-6820	4.7	3600	NHAO	dust phase (re-brightening)	Fig. 11
May 26.72	54 247.22	4160-6820	4.7	3600	NHAO	dust phase (re-brightening)	
Jun. 4.64	54 256.14	4160-6820	4.7	3600	NHAO	dust phase	
Jun. 10.63	54 262.13	4160-6820	4.7	1800	NHAO	dust phase	
2008							
Feb. 7.86	54 504.36	3750-8250	10	2880	FBO	plateau	
Feb. 18.87	54 515.37	4160-6820	4.7	2400	NHAO	plateau	
Feb. 27.78	54 524.28	3750-8250	10	720	FBO	plateau	
Jun. 9.67	54 627.17	4160-6820	4.7	3600	NHAO	plateau	
Jul. 8.58	54 656.08	4160-6820	4.7	2400	NHAO	plateau	
Jul. 30.57	54 678.07	4160-6820	4.7	1800	NHAO	plateau	
Sep. 8.44	54 717.94	4160-6820	4.7	1800	NHAO	plateau	†
Sep. 9.43	54 718.93	4160-6820	4.7	1800	NHAO	plateau	Fig. 12∗
2009							
Apr. 10.80	54 932.30	3900-8200	5	1800	BAO	plateau	Fig. 13
May 9.52	54 961.02	4130-6860	0.1	900	Subaru	plateau	
Jun. 15.52	54 998.02	4130-6860	0.1	600	Subaru	plateau	
Jun. 16.50	54 999.00	4130-6860	0.1	900	Subaru	plateau	
Jun. 26.55	55 009.05	4000-8000	10	900	GAO	plateau	
Jul. 4.46	55 016.96	4130-6860	0.1	900	Subaru	plateau	
Jul. 6.40	55 018.90	4130-6860	0.1	1200	Subaru	plateau	
Sep. 10.44	55 084.94	4000-8000	10	480	GAO	plateau	
Sep. 16.42	55 090.92	4000-8000	10	1260	GAO	plateau	
2010							
Mar. 11.80	55 267.30	4120-9680	10	600	HHAO	plateau	
Mar. 12.80	55 268.30	4000-8000	10	1260	GAO	plateau	Fig. 13
Apr. 17.70	55 304.20	4130-9690	10	900	HHAO	plateau	
Jun. 24.60	55 372.10	4000-8000	10	600	GAO	plateau	
Jul. 1.40	55 378.90	4130-6860	0.1	600	Subaru	plateau	
Jul. 19.53	55 397.03	3700-7500	10	1500	KAO	plateau	Fig. 13
Aug. 1.51	55 410.01	4100-9640	10	900	HHAO	plateau	Fig. 13
2011							
Mar. 17.64	55 638.14	4130-6860	0.1	600	Subaru	plateau	Fig. 14
Apr. 11.14	55 662.64	4470-6890	5	600	Asiago	plateau	Fig. 13
Jun. 12.44	55 724.94	4130-6860	0.1	600	Subaru	plateau	Fig. 14
Jul. 24.28	55 766.78	4130-6860	0.1	600	Subaru	plateau	Fig. 14

Notes. UT: Universal time at start of exposure. ∗ Spectra are shown in the online material. † Data without the flux calibration because of a poor weather condition or missing y-band observation.

Table 5. Equivalent widths of absorption lines and fluxes for emission lines measured in the NHAO spectra.

	2007																	
Date (UT)	Feb. 14.86		Feb. 19.84		Feb. 21.82		Feb. 25.83		Feb. 28.81		Mar. 7.80		Mar. 21.82		Mar. 25.80		Apr. 11.82		May 2.78	
JD - 2 400 000	54 146.36		54 151.34		54 153.32		54 157.33		54 160.31		54 167.30		54 181.32		54 185.30		54 202.32		54 223.28	
ID	abs	em	abs	em	abs	em	abs	em	abs	em	abs	em	abs	em	abs	em	abs	em	abs	em
Hδ 4102					0.90	211.6:		452.0		324.9										
Fe II (27,28) 4173/4178	1.21					101.6:		258.8		232.3		2.62				0.27				
Fe II (27) 4233	0.54					62.4:		161.3		124.7		2.42				0.54				
Fe II (27) 4273	0.28					100.8:		112.1		146.6										
Hγ 4341	3.35				1.15	186.6:		523.7		370.1		3.52				0.97				
Fe II (27) 4417	0.66					74.5:		231.0		129.0										
Fe II (38,37) 4508/4520	0.68											6.48		1.07		1.73				
Fe II (37) 4556												3.92		1.29		1.33				
Fe II (38) 4584												5.03		1.05		1.28				
Fe II (37) 4629												2.15		0.57		0.56				
Hβ 4861	2.61		1.65	114.8	0.79	334.5		988.0		733.9		7.85		1.30		1.57		0.46		
Fe II (42) 4924	0.59	1.61	2.64	91.1	1.28	142.9		313.8		276.2		4.06		0.82		1.07		0.36		
Fe II (42) 5018	0.81	1.48	3.07	79.0	3.51	114.6		366.8		224.9		3.78		0.95		1.16		0.39		
Fe II (52) 5169	1.04	2.15	3.66	34.1	2.85	88.2		281.6		175.7		4.57		0.82		1.17		0.47		
Fe II (49) 5198												1.86		0.36		0.51		0.09		
Fe II (49) 5234	0.60					132.4		297.6		186.0		1.56		0.30		0.42		0.08		
Fe II (49) 5276	0.39					126.6		314.4		257.0		1.74		0.26		0.61		0.24		
Fe II (49) 5317	0.48					98.0		228.0		151.4		2.54		0.47		0.58		0.18		
Fe II (48) 5337	0.68					88.9		137.7		35.9										
Fe II (48) 5363										73.0		0.69				0.13				
Fe II (49) 5425										58.6		0.60				0.12				
Fe II (55) 5535			1.66	11.2						65.2		0.70		0.09		0.15		0.04		
[O I] 5577										42.5		1.41		0.29		0.45		0.13		
[N II] 5755										7.71						0.14		0.11		
He I 5876	0.07																			
Na I D2 5890, D1 5896	2.05		6.80	20.3	10.7	64.0	5.85	140.2	6.00	87.8		2.19		0.52		0.60		0.29		0.18
Fe II (46) 5991										25.0		0.39								
Fe II (74) 6148 , 6149										6.92		0.61		0.08		0.14				
O I 6156, 6157, 6158	0.90		0.99	24.4	0.23	101.9		131.8		52.2										
Fe II (74) 6248	0.26			25.0		68.0		130.4		68.4		1.21				0.21				
unid 6285	0.88		0.90		0.95		1.45													
[O I] 6300										26.7		3.36		1.06		1.39		0.88		0.57
Si II 6347	0.81		1.81	5.43	1.43		0.89													
[O I] 6364										20.3		1.26		0.37		0.49		0.34		0.22
Si II 6371	0.65		0.89	11.3	1.19		0.75													
O I 6454, 6456 / Fe II (74) 6456	0.69		0.97	15.2		58.6		66.9		70.7		0.82		0.13		0.18				
N I 6482, 6483, 6484, 6485	0.71																			
N I 6521																				
Hα 6563	1.77	4.45	3.70	217.9	2.39	637.1	32.0	2200		3304		50.8		10.6		14.3		5.85		1.64
N I 6645	0.19																			
N I 6653	0.22																			
He I 6678	0.03																			
N I 6723	0.22																			

Table 5. continued.

	2007										2008									
Date (UT)	May 7.74		May 20.69		May 26.72		Jun. 4.64		Jun. 10.63		Feb. 18.87		Jun. 9.67		Jul. 8.58		Jul. 30.57		Sep. 9.43	
JD - 2 400 000	54 228.24		54 241.19		54 247.22		54 256.14		54 262.13		54 515.37		54 627.17		54 656.08		54 678.07		54 718.93	
ID	abs	em	abs	em	abs	em	abs	em	abs	em	abs	em	abs	em	abs	em	abs	em	abs	em
Hδ 4102																1.52				1.25
Fe II (27,28) 4173/4178																				
Fe II (27) 4233																				
Fe II (27) 4273																				
Hγ 4341															1.54	1.98		2.42	2.56	3.12
Fe II (27) 4417																				
Fe II (38,37) 4508/4520																				
Fe II (37) 4556																				
Fe II (38) 4584																				
Fe II (37) 4629																				
Hβ 4861				0.54	6.89	1.13						3.06		3.19	0.87	4.24	1.41	4.82	1.70	4.49
Fe II (42) 4924				0.22		0.46		0.13							0.30	0.21	0.44	0.23	0.27	0.38
Fe II (42) 5018				0.42		0.54		0.18							0.19	0.23		0.25	0.15	0.34
Fe II (52) 5169				0.54		0.66		0.23							0.32	0.17	0.30	0.14	0.29	0.19
Fe II (49) 5198																				
Fe II (49) 5234																0.04		0.04		0.08
Fe II (49) 5276																0.10		0.10		0.16
Fe II (49) 5317				0.18		0.21									0.13	0.08		0.09	0.06	0.16
Fe II (48) 5337																				
Fe II (48) 5363																				0.06
Fe II (49) 5425																				
Fe II (55) 5535																0.06		0.05		0.11
[O I] 5577																				
[N II] 5755																0.81		0.74		0.95
He I 5876																0.22		0.24		0.27
Na I D2 5890, D1 5896		0.11	11.6	0.20	9.92	0.32														
Fe II (46) 5991																				
Fe II (74) 6148 , 6149																				
O I 6156, 6157, 6158				0.09																
Fe II (74) 6248				0.04																
unid 6285																				
[O I] 6300		0.36		0.32		0.46		0.48		0.18										
Si II 6347																				
[O I] 6364		0.13		0.12		0.20		0.15		0.08										
Si II 6371																				
O I 6454, 6456 / Fe II (74) 6456																				
N I 6482, 6483, 6484, 6485																				
N I 6521																				
Hα 6563		2.71	2.85	3.18	6.85	5.36		2.64		0.90		13.4		16.2		16.7		21.0		22.9
N I 6645																				
N I 6653																				
He I 6678																0.16		0.20		0.22
N I 6723																				

Notes. The unit of equivalent width is Å. The unit of flux is 10^{-11} erg cm^{-2} s^{-1} Å^{-1}.
: Uncertain value due to the variable weather condition.

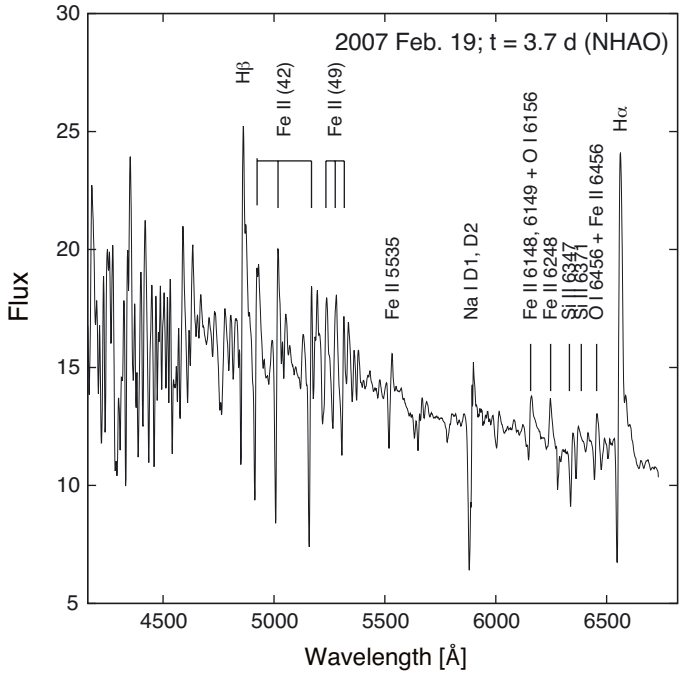

Fig. 7. A spectrum of V1280 Sco on 2007 February 19. The unit of the ordinate is 10^{-11} erg cm^{-2} s^{-1} Å^{-1}.

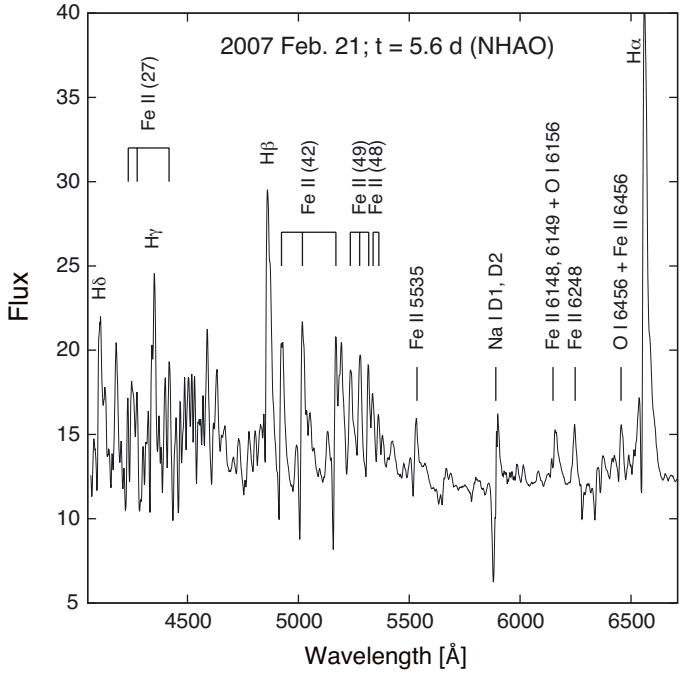

Fig. 8. A spectrum of V1280 Sco on 2007 February 21. The unit of the ordinate is 10^{-11} erg cm^{-2} s^{-1} Å^{-1}.

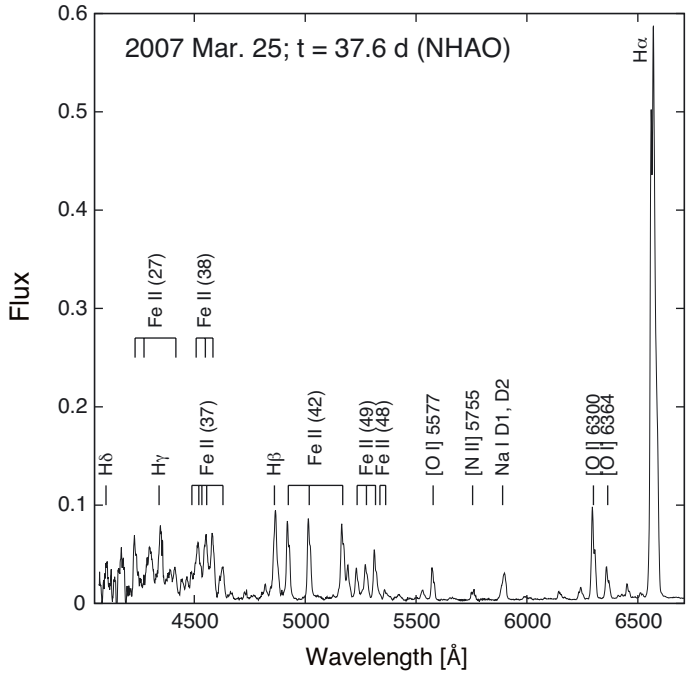

Fig. 10. A spectrum of V1280 Sco on 2007 March 25. The unit of the ordinate is 10^{-11} erg cm^{-2} s^{-1} Å^{-1}.

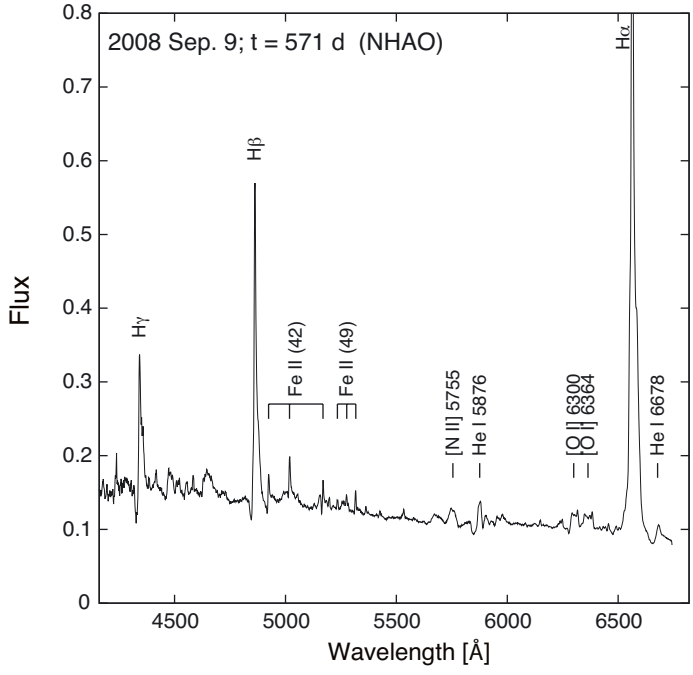

Fig. 12. A spectrum of V1280 Sco on 2008 September 9. The unit of the ordinate is 10^{-11} erg cm^{-2} s^{-1} Å^{-1}.